Available online at www.sciencedirect.com
SCIENCE DIRECT
Thermochimica Acta 443 (2006) 87–92
thermochimica acta
www.elsevier.com/locate/tca

Synthesis and characterization of acidic properties of Al-HMS materials of varying Si/Al ratios

T. Chiranjeevi, G. Muthu Kumaran, J.K. Gupta, G. Murali Dhar *

Indian Institute of Petroleum, Dehradun 248 005, India

Received 15 December 2005; accepted 5 January 2006
Available online 20 February 2006

Abstract

HMS and Al-HMS materials with Si/Al ratio in the range 5–45 were synthesized by neutral templating pathway. The as synthesized as well as calcined samples were examined for pore size distribution, surface area and XRD. These investigations confirmed the hexagonal mesoporous structure formation at all Si/Al ratios. The TGA measurements indicated that two types of template species interacting with Si or Al could be distinguished. The acidity and acid strength distribution studies using microcalorimetric NH_3 adsorption indicated that the acidity increases with Al content in the mesoporous structure. The presence of Al in the structure creates a wide variety of acid sites of varying strengths. The heterogeneity of the sites also increases with Al content of the catalysts. The activities for cumene cracking reaction to test acidity of the materials supported the trend obtained from microcalorimetric NH_3 adsorption results.

Keywords: HMS; Al-HMS; Mesoporous materials; Microcalorimetry; Acidity; Acid strength distribution

1. Introduction

Aluminosilicates like clays and zeolites are well-known in catalyzing various organic transformations that are of industrial interest [1–8]. These materials are limited by their pore size to process bigger molecules [7]. In quest of large pore inorganic structures, Mobil scientists discovered MCM-41 type of materials in which Al can be substituted for silica to yield acidic materials [9–11]. Since then a large number of mesoporous structures were prepared using a wide variety of templates, which enabled variation in pore size, wall thickness, long range order, etc., parameters [12]. Some of the structural types that received considerable attention in recent years are: MCM-41 and its metal ion substituted analogues [13], HMS containing various metal ions [12,13] and substituted MSU and KIT type of materials. Among these materials, Al-MCM-41 and other metal substituted analogues figured in large number of studies [11,14]. In recent years HMS, Al-HMS, Ti-HMS, Al-SBA-15 and other metal substituted SBA-15 structures have also attracted attention [14–19].

Many ions like Al, Ti, V, Zn, Ga, etc., can be substituted into the structures [20,21], however as far as the acidic properties are concerned Al substitution is the most favored one. It is well-known that Al substitution into silicate structure generates Bronsted acidity and these acid sites participate in many industrially important organic transformations [8,14]. In an attempt to prepare better acidic catalysts, synthesis, characterization and evaluation of novel materials containing Al have been investigated. Al-MCM-41 has been extensively studied in this respect and the acidic properties were characterized by Temperature Programmed Desorption (TPD) [20], microcalorimetry [22,23] and IR methods [24]. However, Al-HMS and Al-SBA-15 type of materials received comparatively less attention. There are only limited numbers of studies on Al-HMS type of materials with respect to acidic and catalytic properties [25–27]. Mokaya and Jones [25] used infrared spectroscopic method of pyridine adsorption to elucidate Bronsted and Lewis acid sites. They have concluded that these materials contain Bronsted acid sites that are comparable in acidity to H-Y zeolite. Yue et al. [26] studied acidic properties of Al-HMS of various Si/Al ratios using NH_3TPD and concluded that these materials have comparable acidity in strength and magnitude to H-Y zeolites. These investigations gave interesting results on the nature of acid sites but for complete description of acidic properties

* Corresponding author. Fax: +91 135 2660202.
E-mail address: gmurli@iip.res.in (G.M. Dhar).

0040-6031/$ – see front matter © 2006 Elsevier B.V. All rights reserved.
doi:10.1016/j.tca.2006.01.004

requires the amount of acid sites and also acid strength distribution, since different type of reactions need acid sites of different strength [8]. Microcalorimetry is ideally suited for such measurements [28–30] and has been used to investigate the acid strength distribution in Al-MCM-41 type of materials [23,31]. In order to bridge the gap, in this investigation a series of Al-HMS materials with varying Si/Al ratios between 5 and 45 have been synthesized following the neutral templating pathway and characterized by X-ray diffraction (XRD), thermogravimetric analysis (TGA), solid state NMR and microcalorimetric measurements for evaluation of acidity and acid strength distribution. The acidic functionality was also evaluated using cumene cracking as a test reaction. The discussion on the physico-chemical characterization, acidic properties and their relation with catalytic activities forms the contents of this communication.

2. Experimental

The HMS and Al-HMS materials were synthesized following procedures similar to Pinnavaia and coworkers [32], Mokaya and Jones [25] via neutral templating pathway using hexadecylamine as the surfactant. In a typical synthesis of Al-HMS (Si/Al = 35) material, 0.6 g aluminum isopropoxide was mixed with 35 ml of isopropyl alcohol (IPA) (step-1). 6.03 g of hexadecylamine was mixed with 100 ml of water + 28.5 ml of IPA and was stirred for 30 min (step-2). 20.83 g TEOS was mixed with step-1 solution with the addition of 40 ml of H_2O and stirred for 30 min (step-3). The step-2 solution containing template was mixed with step-3 solution along with 40 ml of H_2O and stirred for 4 h (step-4). The final pH of the solution was 9.3. The step-4 solution was aged for 20 h at room temperature (25 °C) to obtain crystalline product. The solid product was separated by filtration and dried at 110 °C overnight and calcined at 540 °C for 1 h in nitrogen flow followed by calcination in flowing air for 6 h. The materials of various Si/Al ratios were synthesized by taking appropriate amounts of aluminum isopropoxide and TEOS to obtain 5, 15, 25, 35 and 45 Si/Al ratios following the above procedure (Table 1). The calcined mesoporous materials were characterized by XRD using GEXRD-6 Diffractometer and Micromeritics ASAP-2010 adsorption–desorption unit for structure, surface area and pore size distribution analysis. The TGA measurements were carried out using Dupont Model–951 thermogravimetric analyzer at a heating rate of 10 °C min^{-1} under nitrogen flow of 25 ml min^{-1}. ^{29}Si and ^{27}Al MAS NMR spectra of HMS and Al-HMS samples were obtained on a Bruker DRX-300 spectrometer operating at 59.63 and 78.2 MHz, respectively, using a 7 mm Brucker CP/MAS probe. All finely powdered samples were tightly packed into a 7 mm ZrO_2 rotor fitted with kel-F cap and spun at 4.5 kHz. For ^{29}Si MAS spectra, 1 K data points were acquired with a 3.5 μs ($\pi/2$) single pulse excitation with broad band ^1H decoupling (HPDEC) sequence, 10 s relaxation delay, 23 kHz, spectral width and 640 transients were co added for each experiment. Each time domain data were zero filled to 2 K size and Fourier transformed using 50 Hz Gaussian line broadening, spectra were phase corrected in zero and first order followed by base line correction. ^{29}Si chemical shifts were externally referenced to tetra methyl silane (TMS). Each spectrum was deconvoluted using the Bruker software to compute the area of each individual peak with three variable iteration method. Similarly, ^{27}Al MAS NMR of samples was performed using a 0.6 μs ($\pi/12$) single pulse nutation, 1 s delay with 128 transients and 250 kHz spectral widths. Fifty hertz line broadening were used in Fourier transformation. All spectra were zero and first order phase corrected and were externally referenced to $AlCl_3{\cdot}6H_2O$ (ALDRICH).

Microcalorimetric studies of adsorption of ammonia have been performed to determine total acidity and acid strength distribution using a Tian-Calvet type heat flux microcalorimeter (Model C-80 Setaram, France) connected to a volumetric adsorption unit for sample treatment and probe molecule delivery [33]. Samples were preheated at 450 °C under vacuum for 4 h prior to microcalorimetric measurements. The heats evolved from sequential doses of ammonia onto the sample were measured at 175 °C. The heat of adsorption generated for each dose was calculated from the resulting thermograms and the amount of ammonia adsorbed from the initial and final pressures. Sequential doses give the differential heat of NH_3 adsorption as a function of coverage (i.e. differential heat curves). It provides the information about the number and strength of acid sites on samples.

The catalytic activities were determined in a fixed-bed microreactor operating at atmospheric pressure and interfaced with six way sampling valve to a gas chromatograph for on line product analysis. The cumene cracking was carried out at 400 °C in a nitrogen flow at the rate of 40 ml min^{-1}. The first order rates were evaluated according to equation $x = r(W/F)$, where r is rate in mol h^{-1} g^{-1}, x the fractional conversion, W the weight of the catalyst in grams and F is the flow rate of reactant in mol h^{-1}. The conversions were kept below 15% to avoid diffusional limitations [34].

Table 1
XRD and surface area data of HMS and Al-HMS samples

Sample	Gel composition	SBET (m^2 g^{-1})	d (1 0 0) (Å)	a (Å)
HMS	SiO_2:0.25HDA:100H_2O	924	54	62.3
SAR: 5	SiO_2:0.1Al_2O_3:0.25HDA:100H_2O	701	30	34.6
SAR: 15	SiO_2:0.033Al_2O_3:0.25HDA:100H_2O	815	38	43.8
SAR: 25	SiO_2:0.02Al_2O_3:0.25HDA:100H_2O	941	40	46.2
SAR: 35	SiO_2:0.014Al_2O_3:0.25HDA:100H_2O	1050	49	56.5
SAR: 45	SiO_2:0.011Al_2O_3:0.25HDA:100H_2O	1110	54	62.3

SAR, Si/Al ratio of Al-HMS samples; HAD, hexadecylamine.

3. Results and discussion

3.1. X-ray diffraction results

Al-HMS materials with different Si/Al ratios obtained after calcinations were characterized by XRD and sorption techniques for establishing structure and texture. The XRD patterns of Al-HMS are shown in Fig. 1. It can be seen that XRD peak around $d = 4.7$ nm is obtained in all the cases. It can be clearly seen that calcined samples exhibited a single (1 0 0) peak. The XRD patterns are in agreement with the literature reports [25,32,35]. It can be noted that with the increase of Al content the d spacing decreases. The XRD patterns are less sharp and broad with the introduction of more and more aluminum into the structure. This might be due to reduction in hexagonal order. Similar type of behavior was reported for Al-MCM-41 materials [10,36].

3.2. Surface area results

The samples were examined by surface area and pore size distribution (Table 1). It can be seen that surface area decreases with increase of Al into the structure. These results taken together with above discussed XRD data support the above suggestion that hexagonal order is decreasing with the decrease of Si/Al ratio. The materials exhibited a narrow pore size distribution centered on 38 Å [15].

3.3. ^{27}Al, ^{29}Si NMR results

The ^{27}Al NMR spectra of Al-HMS as synthesized as well as calcined are shown in Fig. 2. It can be seen that as synthesized Al-HMS samples exhibit one peak at ∼55 ppm and another very small peak at 0 ppm. The single sharp peak at ∼55 ppm is due to Al in tetrahedral coordination and a weak signal at 0 ppm is due to octahedral aluminum. It can be inferred from the spectra that almost all Al is in tetrahedral coordination suggesting that

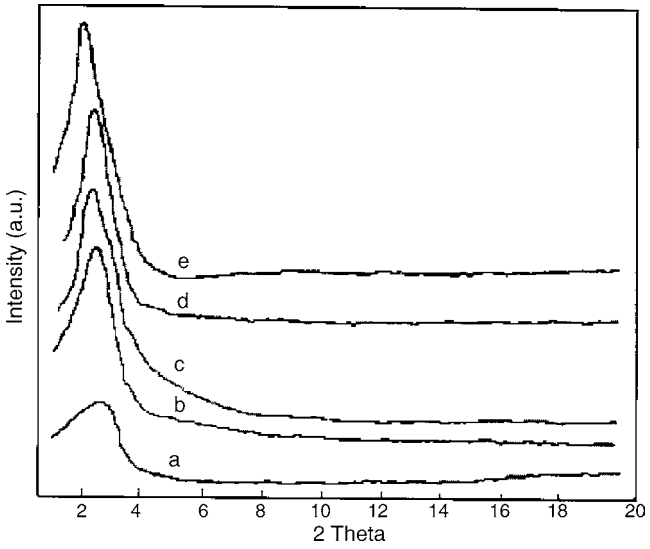

Fig. 1. XRD patterns of Al-HMS material for different Si/Al ratios (a, 5; b, 15; c, 25; d, 35; e, 45).

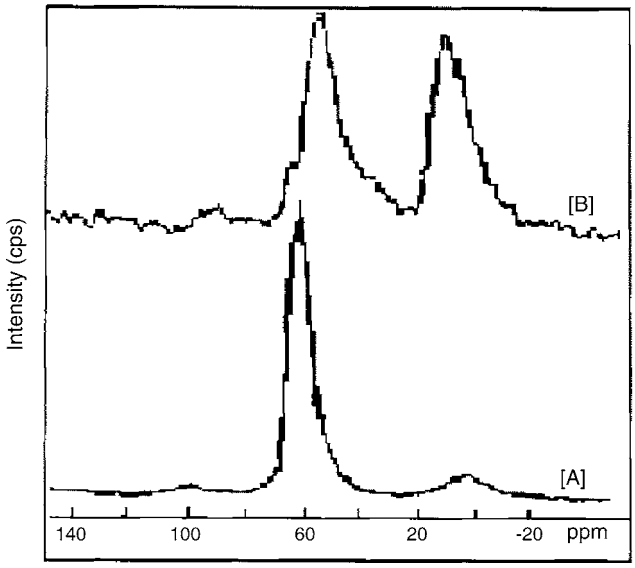

Fig. 2. ^{27}Al MAS NMR spectra of as synthesized (A) and calcined (B) Al-HMS, (SAR: 35) materials.

major part of Al entered into HMS structure (Fig. 2A) during synthesis. However, as can be seen from the spectra (Fig. 2B), the sample exhibits two peaks after calcination due to octahedral and tetrahedral coordination indicating that considerable amount of dealumination occurred during calcination.

The ^{29}Si NMR spectra can be deconvoluted to obtain information on environment of Si and its connectivity [37,38]. The ^{29}Si NMR spectra of Al-HMS materials consists of four well-resolved peaks at −110, −100, −89 and −84 ppm which can be assigned to Q^4 [$Si(SiO_4)$], Q^3 [$Si(SiO_3)OH$], Q^2 [$Si(SiO)_2OH_2$] and Q^1 [$Si(SiO)_1OH_3$] structural units, respectively. The presence of Q^4 units indicates a well-developed three-dimensional framework of Si–O–Si bonds, Q^3, Q^2 and Q^1 peaks indicates the connectivity of Si to hydroxyl groups or Al atoms. The results of deconvolution of ^{29}Si NMR spectra are shown in Table 2. It can be seen that the % Q^4 species is 72% in HMS materials, which decreased to 43% after Al incorporation. This observation also suggests that substantial amount of Al is incorporated into the structure. It can also be noted that calcination increases the Q^4 species, which suggests that considerable dealumination occurred during calcination. These results are in agreement with ^{27}Al NMR results discussed earlier. ^{29}Si, ^{27}Al NMR clearly suggests that substantial amount of Al is in tetrahedral coordination in these Al-HMS materials in as synthesized and calcined materials.

3.4. Thermogravimetric analysis (TGA)

TGA is a useful technique to gain information about the interaction of template with Al and Si atoms present in the mesoporous materials [10,39]. The thermograms of HMS and Al-HMS materials of various Si/Al ratios are shown in Fig. 3. All the spectra were obtained after keeping isothermal at 200 °C before starting the experiment. It can be seen that there is a rapid weight loss in 200–300 °C region in all the samples. However, in the case of Al containing samples there is additional weight

Table 2
Deconvolution data of single pulse ^{29}Si MAS NMR spectra of HMS and Al-HMS samples

Sample	Q^4		Q^3		Q^2		Q^1	
	ppm	%	ppm	%	ppm	%	ppm	%
HMS (uncalcined)	−110	72	−100	28				
Al-HMS (uncalcined)	−111.48	43	−99.2	42.5	−89.9	13	−84.7	1.5
Al-HMS (calcined)	−110.5	62	−101	32.4	−92.0	3.51	−88.0	2.09

loss between 300 and 500 °C region. A small weight loss is also observed in high temperature region. Busio et al. [39] studied Al-MCM-41 with different Si/Al ratios and also observed three regions of weight loss. Mokaya and Jones [25,35] examined the thermograms of Al-HMS and HMS materials as a function of Si/Al ratios and suggested three weight loss regions. They have interpreted 200–300 °C region weight loss as due to interaction of amine with silanol groups on the siliceous part of the HMS and Al-HMS materials. The weight loss between 300 and 500 °C is due to protonated high temperature amine interacting with the Al ions in the structure. The smaller weight loss in high Si/Al ratio materials is also in agreement with these results. The presence of protonated amine was also supported by an IR band at 1510 cm^{-1} [25]. The small weight loss above 500 °C may be attributed to dehydroxylation of the surface. Our results on HMS and Al-HMS materials presented in this investigation are in good agreement with the above interpretation.

3.5. Microcalorimetric NH_3 adsorption

Acidity characterization of zeolites and other aluminosilicates requires the evaluation of number of acid sites, nature of acid sites like Bronsted and Lewis, and acid strength distribution. There are a number of methods for acidity measurements [6,30,40–42]. The nature of acid sites is determined by IR methods using NH_3 or pyridine bases as probe molecules [41]. These measurements are very useful, as it is well-known that many of the organic transformations are dependent on strength of acid sites; for example, *cis–trans* isomerization and double bond isomerization take place on weak acid sites, while intermolecular hydrogen transfer and polymerization take place on acid sites of medium strength and alkylation and catalytic cracking, etc., reactions require sites of high acid strength [8].

Microcalorimetric adsorption of NH_3 is ideally suited for such purpose [28–31]. The acidity and acid strength distributions were determined using heat flow calorimeter attached to a volumetric sorption unit for probe molecule delivery. The differential molar enthalpy as a function of surface coverage for HMS and Al-HMS materials of Si/Al ratios ranging between 5 and 45 are shown in Fig. 4. It can be seen that NH_3 interacts with acid sites and the interaction is heterogeneous with heats of adsorption ranging from 160 to 60 kJ mol^{-1}. The adsorption heats below 60 kJ mol^{-1} may not be of much interest as these sites correspond to reversibly adsorbed species. Therefore, it is likely that the adsorption sites represented by 60 kJ mol^{-1} and above should be of interest for catalysis. It can be seen from the figure (Fig. 4) that heat of adsorption decreases with ammonia coverage monotonically in HMS and other high Si/Al ratio Al-HMS materials. Some well-defined steps can be noticed in the case of aluminum rich samples. The systematic decrease of differential heats observed in present case is as a consequence of interaction of NH_3 with a variety of surface sites exhibiting different strengths. In some cases plateaus are observed which abruptly changes to lower level when interaction with lower level becomes dominant. However, in the present case the decrease of heat of adsorption with coverage is more or less monotonic. To the best of our knowledge there are no reports on acidity of HMS or Al-HMS materials using microcalorimetric NH_3 adsorption.

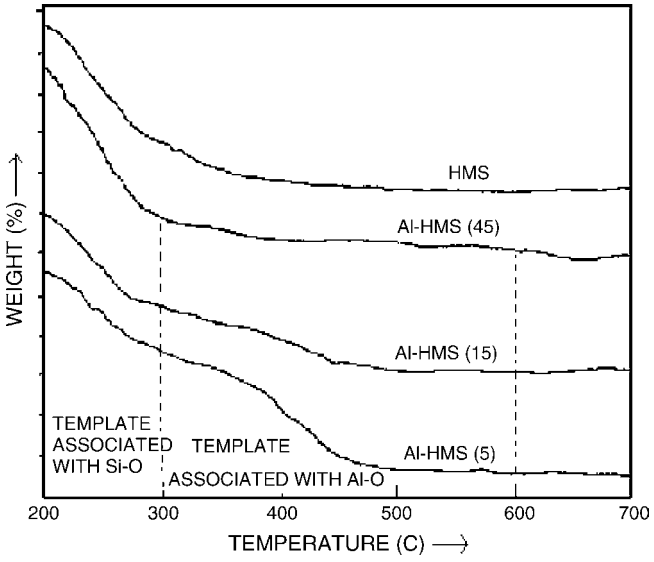

Fig. 3. TGA curves of HMS and Al-HMS materials as a function of Si/Al ratio.

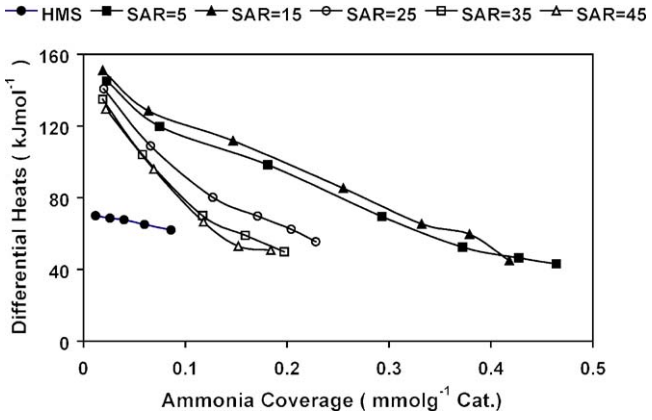

Fig. 4. Differential heats of NH_3 adsorption of various HMS and Al-HMS samples as a function of surface coverage.

However, there are studies using IR pyridine adsorption and TPD of NH_3 [26]. Al-MCM-41 materials have been extensively studied by several authors [23]. It can be seen in Fig. 4 that number of sites available for NH_3 adsorption are lower in HMS material that did not contain any Al in the structure. The differential heat curves of HMS material are characterized by a population of weak acid sites with strength in the range 70–80 kJ mol^{-1}. Introduction of Al into mesoporous silicate framework causes drastic increase in acid site population and their strength. It can be seen that the total acidity decreases with the increase of Si/Al ratio. This is expected since with the increase of Si/Al ratio, the total Al in the structure decreases. Al insertion also increases initial heat values in the range 70–150 kJ mol^{-1}. It can be seen that strong acid sites increase with Si/Al ratio throughout the range of NH_3 coverage except for the sample SAR-5.

The distribution of acidic sites can be better visualized from acid site distribution viz. dn/dq versus q plots. Such a plot for HMS and Al-HMS materials of various Si/Al ratios is shown in Fig. 5, to gain more insight into acid site distribution. It can be noted that HMS material exhibits a peak at ∼70 kJ mol^{-1} only. As the Al is introduced into the structure, a two peak pattern develops at all Si/Al ratios. The first peak centered on 50–80 kJ mol^{-1} suggests the presence of very weak acid sites. The second peak is noticed between 120 and 160 kJ mol^{-1} due to strong acid sites. It can be noticed that the second peak shifts to higher ΔH values with the increase of Al content indicating that acid sites of higher and higher strength are created as more and more Al is introduced into the structure with in the range of Si/Al ratios studied [43,44]. It can also be noticed that there appears another peak in between the above said peaks at around 100–120 kJ mol^{-1} in the case of SAR-15 and SAR-5 samples. It appears that considerable amount of sites of medium acid strength are created in these samples. It is clear that as the Al is introduced into the ordered mesoporous structure, a variety of acid sites with varying strengths are created. In the case of samples containing higher amount of Al, the distribution is more heterogeneous in favor of stronger acid sites.

3.6. Results of cumene cracking reaction

Acidity of the materials can be tested using model compounds. Catalytic cracking of cumene is a well-known test reaction to assess Bronsted acidity. Cumene can be converted on Bronsted acid sites to bring about dealkylation with products benzene and propylene. Cumene can also undergo dehydrogenation to yield α-methyl styrene on Lewis acid sites. In this investigation only trace amounts of α-methyl styrene was observed. This suggests that cumene is almost exclusively converted to benzene and propylene on the Bronsted acid sites present on these Al-HMS materials. The cumene cracking activities expressed as first order rate constant as a function of Si/Al ratio of the Al-HMS material is shown in Fig. 6. It can be seen that cumene cracking activity increases with the increase of Al content in the Al-HMS materials. It can also be noticed that the total acidity also increases in a similar way with the Al content in the material. Similar results were also reported by Yue et al. [26]. Strong Bronsted acid sites efficiently catalyze cumene cracking. It is important to recall that the amount of strong acid sites increase with Si/Al ratio. Mokaya and Jones [25] also noticed an increase of Bronsted acid sites with increase of Si/Al ratio of HMS materials, from their IR adsorption studies using pyridine as the probe molecule. Therefore, it appears that strong Bronsted acid sites are generated as the Al content in the HMS material is increased and these are responsible for the cumene cracking activity. The trend of variation of reactivity as a function of Si/Al ratio is in agreement with acidity variation as determined from microcalorimetric NH_3 adsorption.

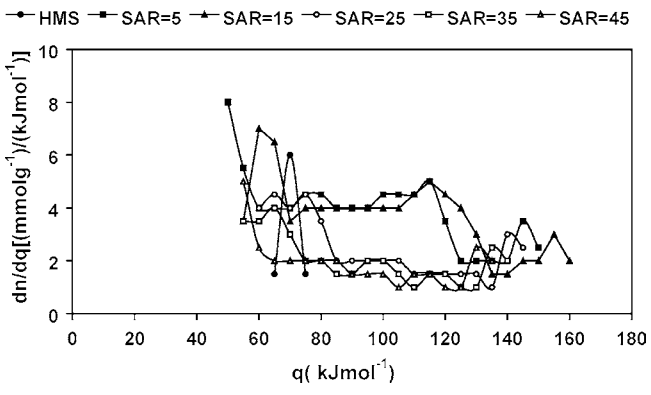

Fig. 5. Acid strength distribution curves of HMS and Al-HMS materials.

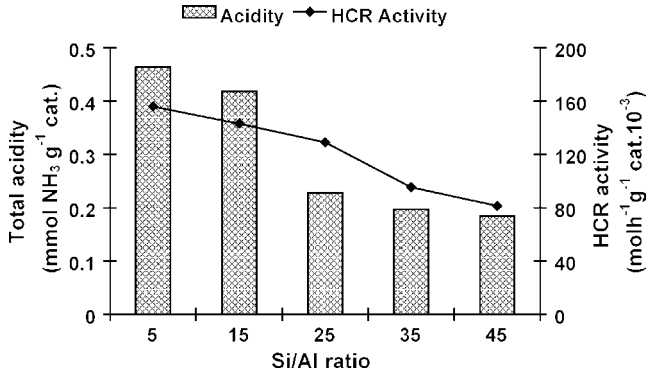

Fig. 6. Variation of acidity and cumene cracking as a function of Si/Al ratio of Al-HMS materials.

4. Summary and conclusions

HMS, Al-HMS mesoporous materials of various Si/Al ratios in the range 5–45, was synthesized using hexadecylamine as surfactant following neutral templating pathway. The as synthesized as well as the calcined samples were examined by X-ray diffraction. The results indicated the formation of hexagonal mesoporous structure. The surface area measurements indicated a decrease of surface area with the increase of Al content. This coupled with the XRD results that the d spacing decreased with increase of Al content suggested a decrease in hexagonal order with Al content. The ^{27}Al, ^{29}Si NMR measurements gave evidence for the presence of significant amount of Al in tetrahedral environment even after calcination at high temperatures. The TGA weight loss as a function of temperature suggested evidence for the presence of two types of hexadecylamine, one

interacting with Si–O groups and the other with Al–O groups. The microcalorimetric acidity measurements indicated that the introduction of Al into HMS structure generates strong acid sites. As the Al content increases the initial heat of NH_3 adsorption was found to increase. The total amount of acid sites decreases with increase of Si/Al ratio of the material. The acid strength distribution indicated that the acid sites are heterogeneous and the heterogeneity increases at higher Al contents in the samples. The cumene cracking activity data indicated only benzene and propylene as reaction products suggesting that the acid sites responsible for the reaction are predominantly Bronsted acid sites. The catalytic activity for cumene cracking exhibited a trend similar to that of variation of acidity as a function of Si/Al ratio.

References

[1] J.A. Rabo, Zeolite Chemistry and Catalysis, ACS Monography, vol. 171, American Chemical Society, Washington, DC, 1976.
[2] J.A. Rabo, G.J. Gajda, Catal. Rev. Sci. Eng. 31 (1989) 385.
[3] P.B. Venuto, E.T. Habib, Fluid Catalytic Cracking with Zeolite Catalysis, Marcel Dekker, Inc., New York, 1978.
[4] P.B. Venuto, Micropor. Mater. 2 (1994) 297.
[5] N.Y. Chen, W.E. Garwood, F.G. Dwyer, Selective Catalysis in Industrial Applications, Marcel Dekker, Inc., New York, 1989.
[6] M. Hunger, Catal. Rev. Sci. Eng. 39 (1997) 345.
[7] A. Corma, Chem. Rev. 97 (1997) 2373.
[8] A. Corma, B.W. Wojciechowski, Catal. Rev. Sci. Eng. 27 (1985) 29.
[9] C.T. Kresge, M.E. Leonowicz, W.J. Roth, J.C. Vartuli, J.S. Beck, Nature 359 (1992) 710.
[10] J.S. Beck, J.C. Vartuli, W.J. Roth, M.E. Leonowicz, C.T. Kresge, K.D. Schmitt, C.T.-W. Chu, D.H. Olson, E.W. Sheppard, S.B. McCullen, J.B. Higgins, J.L. Schlenker, J. Am. Chem. Soc. 114 (1992) 10834.
[11] U. Ciesla, F. Schuth, Micropor. Mesopor. Mater. 27 (1999) 131.
[12] T. Linssen, K. Cassiers, P. Cool, E.F. Vansant, Adv. Colloid Interface Sci. 103 (2003) 121.
[13] A. Tuel, Micropor. Mesopor. Mater. 27 (1999) 151.
[14] D. Trong On, D. Desplantier-Giscard, C. Danumah, S. Kaliaguine, Appl. Catal. A: Gen. 253 (2003) 545.
[15] T. Chiranjeevi, P. Kumar, S.K. Maity, M.S. Rana, G. Murali Dhar, T.S.R. Prasada Rao, Micropor. Mesopor. Mater. 44–45 (2001) 547.
[16] T. Chiranjeevi, P. Kumar, M.S. Rana, G.M. Dhar, T.S.R. Prasada Rao, J. Mol. Catal. A: Chem. 181 (2002) 109.
[17] D. Zhao, Q. Huo, J. Feng, B.F. Chmelka, G.D. Stucky, J. Am. Chem. Soc. 120 (1998) 6024.
[18] A. Vinu, V. Murugesan, W. Bohlmann, M. Hartmann, J. Phys. Chem. B 108 (2004) 11496.
[19] T. Chiranjeevi, G.M. Kumaran, J.K. Gupta, G.M. Dhar, Catal. Commun. 6 (2005) 101.
[20] H. Kosslick, G. Lischke, G. Walther, W. Storek, A. Martin, R. Fricke, Micropor. Mater. 9 (1997) 13.
[21] M.L. Occelli, S. Biz, A. Auroux, Appl. Catal. A: Gen. 183 (1999) 231.
[22] M.L. Occelli, S. Biz, A. Auroux, G.J. Ray, Micropor. Mesopor. Mater. 26 (1998) 193.
[23] J. Janchen, H. Stach, M. Busio, J.H.M.C. van Wolput, Thermochim. Acta 312 (1998) 33.
[24] B. Chakraborty, B. Viswanathan, Catal. Today 49 (1999) 253.
[25] R. Mokaya, W. Jones, J. Catal. 172 (1997) 211.
[26] Y. Yue, Y. Sun, Q. Xu, Z. Gao, Appl. Catal. A: Gen. 175 (1998) 131.
[27] S. Koujout, D.R. Brown, Catal. Lett. 98 (4) (2004) 195.
[28] N.C. Martinez, J.A. Dumesic, Adv. Catal. 38 (1992) 149.
[29] A. Auroux, in: B. Imelik, J.C. Vedrine (Eds.), Catalyst Characterization: Physical Techniques for Solid Materials, Plenum Press, New York, 1994 (Chapter 22).
[30] A. Auroux, Topics Catal. 4 (1997) 71.
[31] A. Auroux, Topics Catal. 19 (3–4) (2002) 205.
[32] T. Tanev, T.J. Pinnavaia, Science 267 (1995) 865.
[33] M. Kumar, F. Aberuagba, J.K. Gupta, K.S. Rawat, L.D. Sharma, G.M. Dhar, J. Mol. Catal. A: Chem. 213 (2004) 217.
[34] M.S. Rana, B.N. Srinivas, S.K. Maity, G.M. Dhar, T.S.R. Prasada Rao, J. Catal. 195 (2000) 31.
[35] R. Mokaya, W. Jones, Chem. Commun. (1996) 981.
[36] Z. Luan, C.F. Cheng, W. Zhou, J. Klinowski, J. Phys. Chem. 99 (1995) 1018.
[37] Z. Luan, C.F. Cheng, H. He, J. Klinowski, J. Chem. Soc. Faraday Trans. 91 (1995) 2955.
[38] C.Y. Chen, H.-X. Li, M.E. Davis, Micropor. Mater. 2 (1993) 17.
[39] M. Busio, J. Janchen, J.H.C. Van Hooff, Micropor. Mater. 5 (1995) 211.
[40] J.K. Gupta, L.D. Sharma, R.P. Mehrotra, T.S.R. Prasada Rao, I. J. Tech. 30 (1992) 77.
[41] S.M. Riseman, F.E. Massoth, G.M. Dhar, E.M. Eyring, J. Phys. Chem. 86 (1982) 1760.
[42] L. Forni, Catal. Rev. Sci. Eng. 8 (1974) 65.
[43] A. Corma, V. Fornes, M.T. Navarro, J.P. Pariente, J. Catal. 148 (1994) 569.
[44] A. Corma, M.S. Grande, V.G. Alfaro, A.V. Orchilles, J. Catal. 159 (1996) 375.